JOM, Vol. 67, No. 10, 2015
DOI: 10.1007/s11837-015-1495-4

Predicting the Crystal Structure and Phase Transitions in High-Entropy Alloys

D.M. KING,[1,2] S.C. MIDDLEBURGH,[2,3,4] L. EDWARDS,[2] G.R. LUMPKIN,[2] and M. CORTIE[1]

1.—Department of Nanomaterials, University of Technology Sydney, Sydney, NSW, Australia. 2.— Institute of Materials Engineering, Australian Nuclear Science and Technology Organisation, Locked Bag 2001Kirrawee DC, NSW 2232, Australia. 3.—Westinghouse Electric AB, Västerås, Sweden. 4.—e-mail: simon.middleburgh@hotmail.com

High-entropy alloys (HEAs) have advantageous properties compared with other systems as a result of their chemistry and crystal structure. The transition between a face-centered cubic (FCC) and body-centered cubic (BCC) structure in the $Al_xCoCrFeNi$ high-entropy alloy system has been investigated on the atomic scale in this work. The $Al_xCoCrFeNi$ system, as well as being a useful system itself, can also be considered a model HEA material. Ordering in the FCC structure was investigated, and an order–disorder transition was predicted at ~600 K. It was found that, at low temperatures, an ordered lattice is favored over a truly random lattice. The fully disordered BCC structure was found to be unstable. When partial ordering was imposed (lowering the symmetry), with Al and Ni limited specific sites of the BCC system, the BCC packing was stabilized. Decomposition of the ordered BCC single phase into a dual phase (Al-Ni rich and Fe-Cr rich) is also considered.

INTRODUCTION

The Al-Co-Cr-Fe-Ni system, and its variations, have attracted a lot of interest since it was first studied at the turn of the century by Huang and Yeh et al.[1–3] Since then, it has been the focus of nearly a quarter of all high-entropy alloy (HEA) studies. This is due to its advantageous properties such as competitive hardness,[4] corrosion resistance,[5,6] wear resistance,[7] and fatigue behavior.[8]

Interestingly, the $Al_xCoCrFeNi$ system is known to transition from a face-centered cubic (FCC) to a body-centered cubic (BCC) crystal structure as the Al content is increased. Extensive studies into the alloying of Al have been performed, and it has been identified that, when there is an Al content of approximately $0 \leq x \leq 0.5$ in the $Al_xCoCrFeNi$ HEA, the crystal structure will remain single-phase disordered FCC.[3,9] At higher Al contents of $0.5 \leq x \leq 0.9$, the system is observed to simultaneously form a BCC-structured phase as well as the FCC structure. Higher Al contents of $0.9 \leq x \leq 1.0$ in $Al_xCoCrFeNi$ result in a single-phase BCC structure being observed.

A number of papers differentiate the BCC phases observed into two types: disordered A2 and ordered B2 forms (the B2 being analogous to the NiAl phase, although the extent of ordering is variable).[4] This effect has been related to the valence electron concentration by Guo et al.[10] Santodonato et al.[11] observed ordering in the $Al_{1.4}CoCrCuFeNi$ system they studied, ascribing the B2 ordering to the Cu-poor phases. Wang et al.[9] also confirmed the existence of the ordered B2 structure in arc-melted samples. The distinctive ordering peak in the x-ray diffraction (XRD) pattern of the HEA, attributed to (100), can actually be seen to some degree in all patterns containing the BCC phase. The (111) peak was clearly observed in the higher-Al-content alloys.

Currently, quantitative understanding of the energetics of this system is lacking. One specific study by Zhang et al.[12] utilized the CALPHAD program to aid in alloy design. Poletti and Battezzati[13] used a number of criteria, both theoretical and experimental, to predict new HEAs and their likely structure. The review by Zhang et al.[14] also highlights some of the atomic-scale methods that are available to study HEAs. The purpose of the

(Published online June 18, 2015)

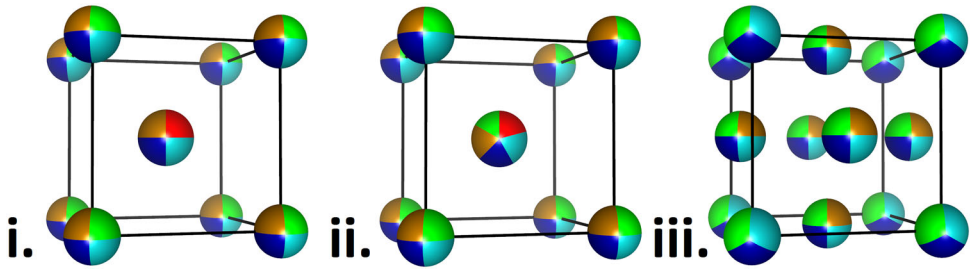

Fig. 1. Ordered structures considered in this work: (i) ordered BCC phase with Al constrained to the center site, (ii) ordered BCC phase with Al constrained to the center site and Ni constrained to the corner site, and (iii) ordered FCC phase with $Pm\bar{3}m$ symmetry. In these models Al is represented in red, Ni is represented in green, and Fe, Co, and Cr are interchangeably gold, light blue, and dark blue.

current study is to use atomic-scale simulation techniques to guide future experimental work and provide a method to understand the role of ordering and configurational entropy in these alloys. Tian et al.[15] performed a similar study to understand the Al_xCoCrFeNi system, using atomic-scale methods to model a range of static systems. The work predicts a change in crystal structure with Al content, highlighting the suitability of the method used in this work, but does not consider the experimentally observed role of ordering in the alloys and the subsequent effect on the configurational entropy term.

METHODOLOGY

Past work[6] utilized a method by which randomly populated FCC supercells were relaxed within the VASP program[16] to understand the drive for Cr segregation in the CoCrFeNi system (an experimentally observed phenomenon[17]). The results of the work compared favorably with experimental results for the system and previous atomic-scale methods using special quasirandom structure (SQS) supercells.[18] This work employs the same random population method as past work.[6] Full geometry optimization was carried out for each supercell, allowing both the atomic positions, shape, and volume of the supercell to vary. The cutoff criterion for the self-consistent field calculations was 1×10^{-4} eV and 1×10^{-3} for the geometry step.

An added complexity in this work is that we investigate the impact of Al ordering and subsequently Al-Ni ordering (see Fig. 1i and ii) on the stability of the BCC phase in comparison with the completely disordered BCC structure. In the ordered B2 structure, the NiAl intermetallic, for example, Al can be thought of as occupying the center site of a body-centered unit cell[19] whilst Ni occupies the remaining site (when simultaneous ordering of both species is investigated).

Ordering of the CoCrFeNi FCC phase in a Cu_3Au ($L1_2$)-type structure[20] (devoid of Al) was also investigated, whereby the Au site is fully occupied by one of the constituent elements (e.g., Fe) and the Cu sites are randomly populated by the remaining species. The Cu_3Au structure has $Pm\bar{3}m$ symmetry, where the Au takes the $1a$ (0,0,0) site and the Cu occupies the $3c$ $(0,\frac{1}{2},\frac{1}{2})$ site (Fig. 1iii).

The stability of the HEA phases was calculated by computing the formation enthalpy from the alloy's constituent metals in their low-temperature structures (i.e., FCC Al, HCP Co, BCC Cr, FCC Fe, and FCC Ni). The FCC HEA supercell is a $2 \times 2 \times 2$ supercell of the FCC unit cell, containing 32 atoms. The BCC supercell is slightly larger: a $3 \times 3 \times 3$ supercell of the BCC unit cell, containing 54 atoms. In both cases a $4 \times 4 \times 4$ γ-centered k-point grid was used with a Methfessel–Paxton smearing method (0.125 eV), providing a suitably low error of $<10^{-3}$ eV per supercell. The pseudopotentials that use the projector augmented wave method provided as part of the VASP package[21] were used with the generalized gradient approximation (GGA)–Perdew–Burke–Ernzerhof (PBE) exchange correlation (using the highest valence electron number available). Spin-polarization effects were considered (as they were in past work[6,22]) to allow the significant magnetic effects to be properly accounted for in the calculated enthalpies.

Each arrangement was repeated 10 times with any erroneous high-energy supercells discounted and the calculation repeated. In all cases, the energies of similar supercells varied by less than ± 0.02 eV per atom, suitable for this study.

To investigate the role of configurational entropy on the systems' stabilities, we use Boltzmann's equation[23] for the configurational entropy (entropy of mixing):

$$\Delta S_{\text{conf}} = k_{\text{B}} \ln \Omega, \tag{1}$$

where k_{B} is Boltzmann's constant and

$$\Omega = \frac{N_{\text{tot}}!}{N_1! N_2! \ldots N_j!}, \tag{2}$$

where

$$N_{\text{tot}} = \left(\sum_{i=1}^{j} N_i \right) \tag{3}$$

for N number of atoms of element i in a j-element system.

Applying Stirling's approximation[24] for $\ln N!$ when $N \gg 1$:

$$\Delta S_{\text{conf}} = -nR\sum_{i=1}^{j} x_i \ln(x_i), \tag{4}$$

since N_i/N_{tot} corresponds to the atomic concentration, x, of element i, $k_B = R/N_A$, where N_A is Avogadro's number and $N_{\text{tot}} = nN_A$, where n is the number of moles.

For a system with partial ordering, we can expand $n_{\text{tot}} = \Sigma_{k=1}^{l} n_k$, where the total number of moles n_{tot} is the sum of the number of moles n of sublattice k for l number of sublattices. Therefore,

$$\Delta S_{conf} = -R\left[\sum_{k=1}^{l} n_k \sum_{i=1, i\neq m}^{j} x_{i,k}\ln(x_{i,k})\right], \tag{5}$$

where m is any element that is not included on sublattice k.

To explore the impact of ordering on the expected experimental observations, Crystal Maker software was used to generate simulated x-ray diffraction patterns.[25] The relaxed structures are mixed with equal weighting within the program and given an instrumental broadening value of 0.02°.

RESULTS

Relaxed Structures

The disordered supercells that were built with FCC symmetry retained their structure through the atomic-scale optimization routine, regardless of Al content. The lattice parameter was observed to vary with Al concentration, as is expected given the larger metallic radius of Al (1.43 Å[26]) compared with the other constituent elements (1.25 Å, 1.36 Å, 1.26 Å, and 1.24 Å for Co, Cr, Fe, and Ni, respectively[26]). The lattice parameter for FCC Al_xCoCrFeNi was predicted to increase from 3.519 Å to 3.556 Å corresponding to $x = 0 \rightarrow 0.57$, a difference of 0.037 Å. The experimental variation in lattice parameter, observed by Wang et al.[9] was 0.025 Å between $x = 0 \rightarrow 0.5$.

The simulated x-ray diffraction patterns for the four FCC Al_xCoCrFeNi systems simulated are given in Fig. 2. The wavelength of the simulated x-rays was set to 1.5406 Å (to match with the majority of experimental data). The main (111) peak (at ~45°) shifts from higher to lower angle as the Al content is increased, as expected, whilst the (200) peak (at ~50°) diminishes in intensity compared with the (111) peak to the theoretical composition of $x = 2.40$ (experimentally, the two higher-Al-content systems are not observed to be FCC).

When the ordered, pseudo-Cu_3Au-type structure of the CoCrFeNi phase is considered (as was predicted by Niu et al.[22] using SQS methods), there are no significant differences in the XRD patterns produced, apart from a very small ordering peak

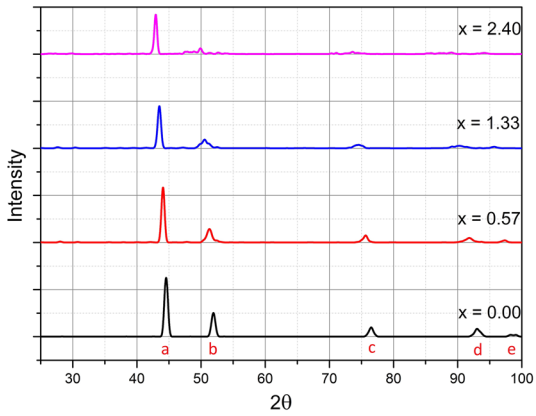

Fig. 2. Simulated x-ray diffraction patterns of FCC Al_xCoCrFeNi with $x = 0.00$, 0.57, 1.33, and 2.40. The peaks are indexed as follows: (a) (111), (b) (200), (c) (220), (d) (311), and (e) (222).

observed at ~36° related to the (110) direction, when each of the four constituent elements are ordered on the Au site. The lattice parameter for the Fe-ordered system (energetically the most stable, as discussed in the following section) is slightly increased to 3.521 Å compared with 3.519 Å in the fully disordered system.

Somewhat surprisingly, the supercells that were built with BCC symmetry without ordering relaxed to a wide variety of simple structures (involving simple movements of the atomic positions away from the ideal BCC sites). At low Al concentrations of $x = 0.00$ and $x = 0.15$, more than 50 % of the structures relaxed to a $R\bar{3}m$ symmetry (hexagonal, not cubic). At intermediate Al contents of $x = 0.50$ and $x = 0.91$, the structures again relaxed to a range of structures: 40 % remained BCC with $Im\bar{3}m$ symmetry, 25 % relaxed to the $R\bar{3}m$ symmetry observed for lower Al contents, 10 % transformed to a FCC $Fm\bar{3}m$ symmetry, while the remainder transformed to lower symmetries of $Fmmm$ and $IA\bar{3}d$. At high Al concentrations, the majority (70 %) of the structures relaxed to an FCC $Fm\bar{3}m$ symmetry with the remainder adopting $R\bar{3}m$ and $Im\bar{3}m$. It is clear that the simple, disordered BCC phase is not the stable structure when predicted using static density functional theory (DFT). It should be noted that, although the structures relaxed preferentially from the initial random BCC arrangement, none of the relaxed systems' energies were lower than the completely random FCC structure (unless it relaxed to the FCC structure). As such, further investigations into these unfavorable systems were not pursued in this work.

Past work[9] experimentally suggested that, when the Al positions in the BCC phase are limited to the center site of the unit cell (preventing Al–Al nearest neighbors), the BCC structure is stabilized. When limiting the positions of the Al, we find that, at low Al concentrations of $x = 0.15$ and $x = 0.50$, the hexagonal ($R\bar{3}m$) phase continued to form for 30 % of the supercells, with the remainder remaining

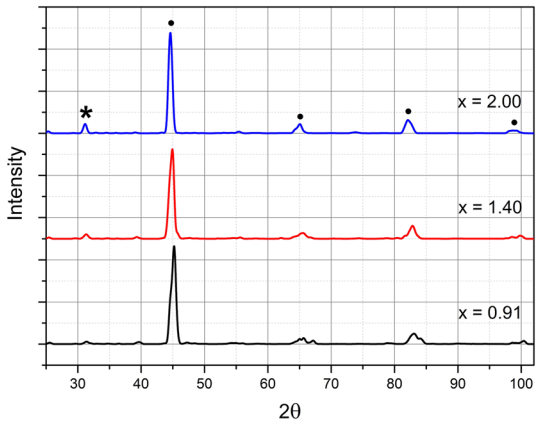

Fig. 3. Simulated x-ray diffraction patterns of BCC $Al_xCoCrFeNi$ with x = 0.91, 1.40, and 2.00. Peaks labeled with the • symbol are the ideal BCC peaks [from low to high angle these are indexed as (110), (200), (211), and (200)], while the ∗ indicates the (100) ordering peak.

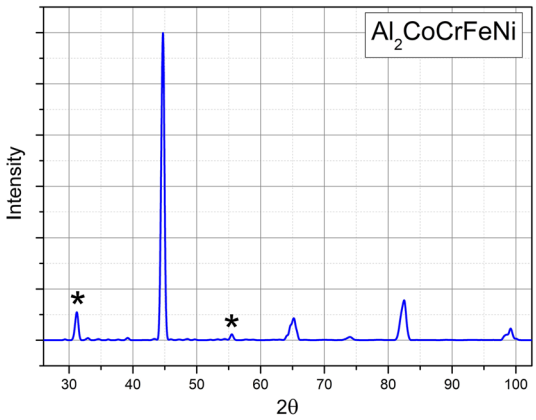

Fig. 4. Simulated x-ray diffraction pattern of BCC $Al_2CoCrFeNi$ with simultaneous ordering of Al and Ni on separate sublattices. The ∗ symbols highlight the experimentally observed ordering peaks.[9]

BCC ($Im\bar{3}m$). For the three higher concentrations of Al considered, all supercells remained in the BCC ($Im\bar{3}m$) symmetry. This is a significant finding that suggests that the atomic-scale ordering (or at least partial ordering of the constituent elements, in this case Al) is a pivotal property required in the formation of the single-phase BCC $Al_xCoCrFeNi$ HEA.

The simulated x-ray diffraction patterns for the Al-ordered BCC systems with the three highest Al concentrations (that showed no relaxations to an alternate symmetry) are shown in Fig. 3.

The peaks normally associated with the BCC phase are highlighted with • symbols and remain for all patterns. A peak at ~31° is prominent in the pattern for the higher Al content (highlighted with the ∗ symbol). This peak is present in the two systems with lower Al content, but the peak is weaker. Wang et al.[9] attributed this peak to (100) and another peak at ~55° to (111), peaks that only form in the ordered structure. The peak at (100) appears in our models as a result of the Al ordering resulting in this regular plane corresponding to a spacing of ~3 Å.

When simultaneous ordering of Al and Ni on two separate sublattices is considered, the systems with high Al concentrations remain BCC in nature, with the two systems with lower Al content morphing into the hexagonal system in 30 % of cases (similar to the Al-ordered systems). The XRD pattern for the highest-Al-content Al-Ni-ordered system is shown in Fig. 4.

The compositions with x = 1.4 and x = 0.9 were similar to the x = 2.0 composition, except for the small shift associated with the change in lattice parameter (0.02 Å between x = 0.9 and x = 2.0). The ordering peak associated with (100) that was observed in the Al-ordered systems remained in these systems, in addition to the experimentally observed peak at ~55°, which is clearly visible in all of the Ni-Al-ordered systems.

Phase Stability

The energy of the disordered CoCrFeNi FCC phase, compared with the partially ordered (Cu_3Au-like) phase, was also considered. It was found that, when Fe was ordered (fully occupying the 1a site), the formation energy per atom dropped to ~0.00 eV, 0.03 eV lower than the fully disordered FCC arrangement. Ni and Cr ordering also lowered the formation enthalpy relative to the fully disordered system by 0.02 eV and 0.01 eV, respectively. The preference in formation enthalpy for the ordered structure, although significant, may be negated by the variation in entropy with temperature. Although vibrational entropy and other forms of entropy will play a role in the phase stability, the configurational entropy is expected to dominate the discrepancy between the fully disordered and the partially ordered phase, as other forms of entropy are expected to cancel out between products and reactants to a greater extent (especially in the absence of a change in state.[27])

A value of $\Delta S_{mix} = 7.19 \times 10^{19}$ eV/K/mol was calculated for the fully disordered system, while the ΔS_{mix} for the partially ordered system is 4.28×10^{19} eV/K/mol. The partially ordered system's configurational entropy was calculated using Eq. 5. The entropy contribution of the completely filled Fe sublattice equated to 0 eV/K/mol as $\ln(1) = 0$. Combining the enthalpies of formation with the configurational entropy term allows the estimation of the Gibbs free energy. Figure 5 reports the Gibbs free energy variation with temperature for the fully disordered and partially ordered CoCrFeNi system. There is a clear crossover at ~600 K, indicating a change in preferential formation. At high temperatures the fully disordered high-entropy alloy is predicted to be favored over the partially ordered system.

The ordering we have considered in this work is very basic, and there are many other forms of atomic ordering that should be considered,

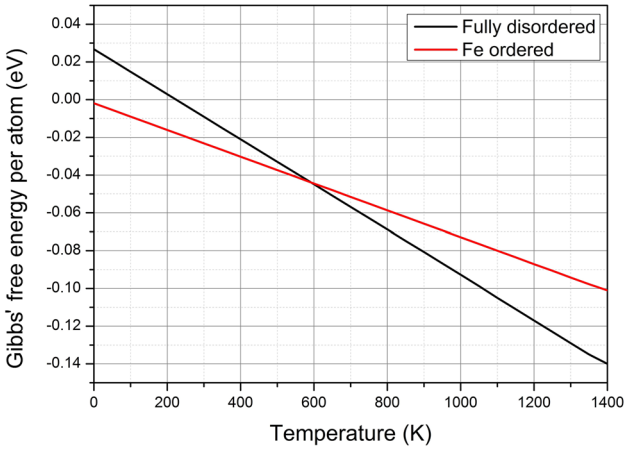

Fig. 5. Calculated variation in Gibbs free energy of the disordered and partially ordered (Fe-ordered) CoCrFeNi systems.

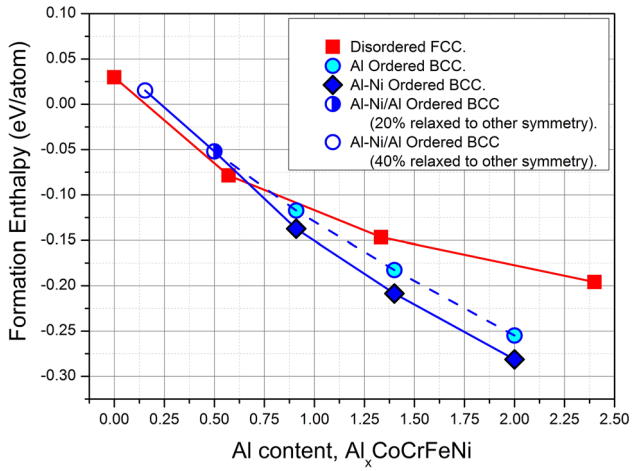

Fig. 6. Variation in formation enthalpy of Al$_x$CoCrFeNi from the constituent elements. Completely disordered face-centered cubic (red), Al-ordered body-centered cubic (light blue), and Ni-Al-ordered body-centered cubic (blue) are plotted. The values for completely disordered body-centered cubic are not included as the simulation predicted this phase to be unstable at all Al contents.

including investigating structures with increased periodicity and complexity. The Cu_3Au structure is merely one example of a possible ordered structure that is more stable in the present instance than a disordered one, and it is possible that some other, as yet identified, ordered structure could be even more stable. Any structure found with a lower enthalpy of formation may still form a completely disordered structure at high temperature (as we predict for the Cu_3Au structure), although the transition point may be higher.

The stability of the Al$_x$CoCrFeNi phases is now investigated: Fig. 6 reports the formation energies of the disordered FCC phase and the ordered BCC phases (both Al and Al-Ni ordered) as a function of Al content. There is a clear change in behavior associated with increasing the Al content that matches extremely well with experimental observations. Between $x = 0.57$ and $x = 0.91$, the calculations predict that preferred symmetry changes from FCC to an ordered BCC phase, and Wang et al.[9] observed this transformation to occur between $x = 0.5$ and $x = 0.9$. As the transition is not observed to be very energetically sharp, the formation of a dual phase (FCC and BCC) can be expected (and is experimentally observed). Entropic considerations mean that the transition point will vary with temperature as there is a discrepancy between the partially ordered BCC system and the fully disordered FCC system. As such, the transition point will shift towards higher Al content with increasing temperature. The current method is not able to probe the subtle variations in composition near the transition point.

The enthalpies of formation for the Al-ordered and the Al-Ni-ordered BCC phases were very similar at low Al concentrations (and combined in Fig. 6). At higher Al contents, there is a notable divergence in stability (although both are more stable than the associated FCC system). The configurational entropy of the Al-Ni-ordered system is similar to the Al-ordered system, and the enthalpy difference is large enough to prevent the predicted change in preference between the formation of the systems with temperature.

Some experimental compositions, mainly studying thermally aged compositions, have found notable cosegregation of Ni with the Al leaving a Cr-Fe-rich phase.[28] This is briefly investigated by considering the following reaction from the single-phase $x = 1.4$ composition forming an Al-Ni-rich and corresponding poor phase in similar stoichiometries to those reported by Wang et al.[28]:

$$Al_{28}Co_{20}Cr_{20}Fe_{20}Ni_{20} \rightarrow Al_7Co_{14}Cr_{14}Fe_{14}Ni_5 + Al_{21}Co_6Cr_6Fe_6Ni_{15}. \quad (6)$$

These compositions are idealized compositions similar to the $Al_{1.5}$ composition measured by Wang et al.[9] The compositions do not vary more than 10 at.%, compared with the experiment; however, as a result of this discrepancy, care should be taken when directly comparing these theoretical results with experiment.

The Al atoms are once again limited to the body-centered site, maintaining the B2 structure, while the Ni atoms are limited to the remaining site of the BCC unit cell (providing the additional ordering calculated to be favorable). The energy released as a result of the partition is 0.01 eV per atom, meaning a dual phase is stable with regards to the enthalpy of the system. From the data we predict that the configurational entropy of the single phase will overcome the enthalpy advantage of the dual phase for the $x = 1.4$ composition at 1250 K. Experimental observations by Wang et al.[28] show a dual phase when quenching from 1373 K; therefore our predictions, which do not consider the other forms of

entropy, should be treated with caution (although a transition from single to dual phase can be expected before the melting point at ~1650 K).

CONCLUSION

Our calculations predict a transition between an FCC-based structure from $0 \leq x \leq 0.75$, to the partially ordered BCC structure with greater Al content. This result closely agrees with the experimentally observed transition from FCC to BCC with Al content in a number of works.

Ordering of the FCC phase was found to be preferable at lower temperatures; our simulations suggested a Cu_3Au-type structure (in a similar manner to work by Niu et al.[22]) The XRD patterns obtained from the simulated supercells match well with experimental data. The transition between ordered and disordered FCC formation was predicted by taking account of the difference in the two systems' configurational entropy. The transition temperature was estimated to be ~600 K; however, other forms of as-yet-unidentified ordering may in reality provide an even more stable structure and hence increase the transition temperature (the formation of which could possibly be kinetically hindered).

It is clear that the fully disordered BCC system (termed the A2 configuration in the Strukturbericht designation) is not stable, as the geometry optimization process relaxed >50 % of the simulated structures to $R\bar{3}m$ and $Fm\bar{3}m$ symmetries (amongst others), a result that would be experimentally obvious. This work predicts that, for a phase with BCC packing to be stabilized, it is necessary for the system to be partially ordered. Here we have shown that Al occupying a single site of the BCC lattice stabilizes the BCC phase and that additional ordering of the Ni in the same structure stabilizes the system further. The associated XRD patterns for the ordered BCC systems match with experimental results, the Al-Ni-ordered system clearly presenting the two experimentally observed ordering peaks at ~31° and ~55°.

The decomposition of the single-phase ordered-BCC structure to a dual-phase structure was investigated for the $x = 1.4$ composition. The calculations predict that a dual-phase structure is favored on enthalpy grounds, but when the configurational entropy terms are considered, estimating the Gibbs free energy of the system, a transition temperature of 1250 K is predicted, above which a single-phase structure is expected. This may be related to the observed transition in the hardness of BCC alloys observed by Wang et al.[28] The simulated transition is extremely indistinct (the entropy terms for the single and dual phases are similar), and therefore the error on the temperature is high and the predicted temperature should be treated with some caution.

ACKNOWLEDGEMENT

This research was undertaken with the assistance of resources provided at the NCI National Facility systems at the Australian National University through the National Computational Merit Allocation Scheme supported by the Australian Government. This work was supported by the Multi-modal Australian ScienceS Imaging and Visualisation Environment (MASSIVE) (https://www.massive.org.au).

REFERENCES

1. K.H. Huang, *A Study on the Multicomponent Alloy Systems Containing Equal-Mole Elements* (Master's thesis, National Tsing Hua University, Hsinchu, Taiwan, 1996).
2. J.W. Yeh, S.K. Chen, S.J. Lin, J.Y. Gan, T.S. Chin, T.T. Shun, C.H. Tsau, and S.Y. Chang, *Adv. Eng. Mater.* 6, 299 (2004).
3. H.P. Chou, Y.S. Chang, S.K. Chen, and J.W. Yeh, *Mater. Sci. Eng. B* 163, 184 (2009).
4. Y.F. Kao, T.J. Chen, S.K. Chen, and J.W. Yeh, *J. Alloys Compd.* 488, 57 (2009).
5. C. Lin, and H. Tsai, *Intermetallics* 19, 288 (2011).
6. S.C. Middleburgh, D.M. King, G.R. Lumpkin, M. Cortie, and L. Edwards, *J. Alloys Compd.* 599, 179 (2014).
7. J.M. Wu, S.J. Lin, J.W. Yeh, S.K. Chen, Y.S. Huang, and H.C. Chen, *Wear* 261, 513 (2006).
8. M.A. Hemphill, T. Yuan, G.Y. Wang, J.W. Yeh, C.W. Tsai, A. Chuang, and P.K. Liaw, *Acta Mater.* 60, 5723 (2012).
9. W.R. Wang, W.L. Wang, S.C. Wang, Y.C. Tsai, C.H. Lai, and J.W. Yeh, *Intermetallics* 26, 44 (2012).
10. S. Guo, C. Ng, J. Lu, and C.T. Liu, *J. Appl. Phys.* 109, 103505 (2011).
11. L.J. Santodonato, Y. Zhang, M. Feygenson, C.M. Parish, M.C. Gao, R.J. Webber, J.C. Neuefiend, Z. Tang, and P.K. Liaw, *Nat. Commun.* 6, 5964 (2015).
12. C. Zhang, F. Zhang, S. Chen, and W. Cao, *JOM* 64, 839–845 (2012).
13. M.G. Poletti, and L. Battezzati, *Acta Mater.* 75, 297–306 (2014).
14. Y. Zhang, T.T. Zuo, Z. Tang, M.C. Gao, K.A. Dahmen, P.K. Liaw, and Z.P. Lu, *Mater. Sci.* 61, 1–93 (2014).
15. F. Tian, L. Delczeg, N. Chen, L.K. Varga, J. Shen, and L. Vitos, *Phys. Rev. B* 88, 085128 (2013).
16. G. Kresse, and J. Hafner, *Phys. Rev. B* 47, 558 (1993).
17. A.K. Singh, and A. Subramaniam, *J. Alloys Compd.* 587, 113–119 (2014).
18. A.J. Zaddach, C. Niu, C.C. Koch, and D.L. Irving, *JOM* **65**, 1780 (2013).
19. R.E. Voskoboinikov, G.R. Lumpkin, and S.C. Middleburgh, *Intermetallics* 32, 23 (2013).
20. P. Ramdohr, *Fortschritte der Mineralogie* 28, 69 (1949).
21. G. Kresse, and J. Hafner, *Phys. Rev. B* 49, 4251 (1994).
22. C. Niu, A.J. Zaddach, A.A. Oni, X. Sang, J.W. Hurt III, J.M. LeBeau, et al, *Appl. Phys. Lett.* 106, 161906 (2015).
23. R. Swalin, *Thermodynamics of Solids* (Wiley, New York, 1991), p. 21.
24. W. Feller, *An Introduction to Probability Theory and Its Applications* (Wiley, New York, 1971).
25. D.J.M. King, S.C. Middleburgh, A.C.Y. Liu, H.A. Tahini, G.R. Lumpkin, and M.B. Cortie, *Acta Mater.* 83, 269 (2015).
26. L. Pauling, *J. Am. Chem. Soc.* 69, 542 (1947).
27. S.C. Middleburgh, K.P.D. Lagerlof, and R.W. Grimes, *J. Am. Ceram. Soc.* 96, 308–311 (2013).
28. W.R. Wang, W.L. Wang, and J.W. Yeh, *J. Alloys Compd.* 589, 143 (2014).